

can be shown by means of ray theory that the propagation time depends on angle θ_1 according to

$$t_i(\theta_1) = \frac{1}{\cot \theta_1 + \cot \theta_2 + \dots + \cot \theta_i} t_0 \quad (7)$$

$i = 1, 2, \dots, N$

where $t_0 = n_1 z/c$ is the propagation time of the ray along the axis, and the angles $\theta_2, \theta_3, \dots, \theta_i$ can be related to θ_1 according to

$$\cos \theta_k = \frac{n_1}{n_k} \cos \theta_1 \quad (8)$$

Let us introduce the angular distribution of light intensity $I(\theta_1)$ such that

$$I(\theta_1) = \frac{dE(\theta_1)}{d\theta_1} \quad (9)$$

where $E(\theta_1)$ is the pulse energy emitted in the cone determined by the angle θ_1 . In order to calculate the moments of eqn. 4, we can substitute the integration over t with integration over θ_1 and obtain

$$M_0 = \int_0^{\theta_{1c}} I(\theta_1) d\theta_1$$

$$M_1 = \sum_{i=1}^N \int_{\beta_i}^{\beta_{i+1}} t_i(\theta_1) I(\theta_1) d\theta_1 \quad (10)$$

$$M_2 = \sum_{i=1}^N \int_{\beta_i}^{\beta_{i+1}} t_i^2(\theta_1) I(\theta_1) d\theta_1$$

where

$$\beta_i = \arccos(n_i/n_1) \quad (11)$$

For a surface-emitter (Burrus type) i.e.d. we can calculate $I(\theta_1)$ from

$$I(\theta_0) = I_m \cos \theta_0 \sin \theta_0 \quad (12)$$

with

$$\sin \theta_0 = \frac{n_1}{n_0} \sin \theta_1 \quad (13)$$

For the following calculations we assumed $n_1 = 1.5$ and $n_0 = 1$. Other types of common optical sources such as edge-emitter i.e.d.s and laser diodes have radiation patterns asymmetrical and more directional. But for small angles of acceptance of optical fibre, i.e. small Δ , the results are expected to be quite similar to that obtained with eqn. 12. For instance, we assumed $I(\theta_0) = I_m \cos^2 \theta_0 \sin \theta_0$ (more directional beam) and obtained results which differ negligibly from those obtained with eqn. 12.

Now, using the assumptions, eqns. 2, 3 and 12 and eqns. 5-7 and 10, we calculate the ratio of the pulse widths for a fibre with N core layers and a fibre with one core layer, i.e. σ_N/σ_1 as a function of the parameter α . (In eqn. 3 we assumed $\Delta = 0.01$, but the variations of this parameter give negligible effect on the results). The obtained curves are plotted in Fig. 2 for $N = 2, 3, 4$ and 8. From these curves we see that significant reduction in pulse dispersion can be expected even with a low number of cores. It is interesting that the optimal value of α , for which we obtain the minimal pulse broadening σ_N , is much smaller than that obtained for graded-index fibres, but it is increasing with the increase of the number of layers. It should be pointed out also that the minima of the curves are broad, i.e. variations of n_i around optimal values would not cause serious increase in pulse broadening.

Therefore we can conclude that multilayer fibres offer significant increase in information capacity of the fibre compared to step-index fibres, even with low numbers of layers, together with low requirements in the precision of fabrication. Hence multilayer fibres may be quite useful for bit rates somewhat higher than step-index fibres would allow.

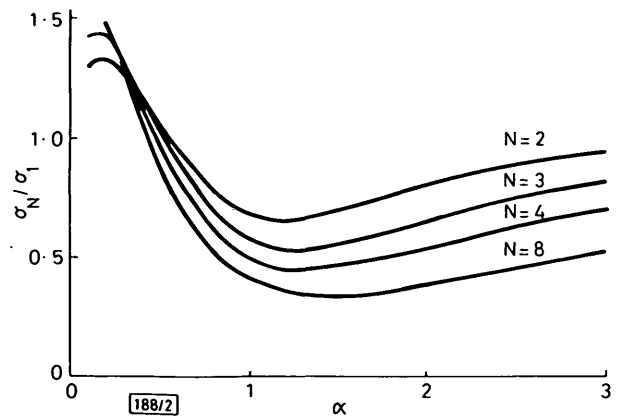


Fig. 2 Ratio of pulse broadening for fibres with N core layers and one core layer as a function of parameter α defined in eqn. 3

Acknowledgment: The author is grateful to Prof. G. Lukatela for encouragement and helpful discussions.

R. PETROVIĆ

15th May 1980

Faculty of Electrical Engineering
18000 Niš, Yugoslavia

References

- 1 KAWAKAMI, S., and NISHIDA, S.: 'Characteristic of a doubly clad optical fiber with a low-index inner cladding', *IEEE J. Quantum Electron.*, 1974, **QE-10**, pp. 879-887
- 2 BELANOV, A. S., DIANOV, E. M., EZHOV, G. I., and PROKHOROV, A. M.: 'Propagation of normal modes in multilayer optical waveguides: I. Component fields and dispersion characteristics', *Sov. J. Quantum Electron.*, 1976, **6**, pp. 43-50

0013-5194/80/140562-02\$1.50/0

MIXED COMPLETE PADE MODEL REDUCTION: A USEFUL FORMULATION FOR CLOSED LOOP DESIGN

Indexing terms: Linear systems, Modelling

A simple formulation for derivation of reduced order models for linear time invariant systems by mixed complete Padé approximation is presented. Various reduced order models of the same order with different combinations of the number of matched Markov parameters and time moments can be derived by equations that resemble the simple Padé equations for approximation at a single point. The advantages of obtaining models by a complete Padé approximation is emphasised.

Many methods for reducing high order linear time invariant systems obtain lower order models that approximate the system in the Padé sense.¹ Let $H(s)$ be the transfer function of the system with expansions about $s = 0$, $s = \infty$ given by

$$H(s) = H_0 + H_1 s + H_2 s^2 + \dots \quad (1)$$

$$H(s) = M_1 s^{-1} + M_2 s^{-2} + M_3 s^{-3} + \dots \quad (2)$$

A linear n th order transfer function

$$G(s) = \frac{\alpha_0 + \alpha_1 s + \dots + \alpha_{n-1} s^{n-1}}{\beta_0 + \beta_1 s + \dots + \beta_n s^n} \quad (\beta_0 = 1) \quad (3)$$

is an $[n-1, n]_L^K$ Padé approximation (p.a.) if its first terms of expansion about $s = 0$ and $s = \infty$ are the first K and L terms of eqns. 1 and 2, respectively. The case $K = 0$ ($L = 0$) represents pure p.a. at $s = 0$ ($s = \infty$), whereas the case of $K, L > 0$ represents mixed p.a.s. An $[n-1, n]_L^K$ with $K + L = 2n$ uniquely defines $G(s)$ for given n and K ($K = 0, 1, \dots, 2n$) and represent a complete p.a., this being distinguished from the various $K + L < 2n$ cases of partial p.a.s.

The terms H_i and M_i are known as the time and Markov parameters of the system. They are related to the state space representation of $S(A, B, C)$ by

$$H_i = CA^{-(i+1)}B; \quad M_i = CA^iB \quad (i = 0, 1, \dots) \quad (4)$$

They are also proportional to the time moments and time series expansion about zero of the system impulse response, respectively. Padé type approximations for model reduction have been treated by many authors using continued fraction expansions, time moment matching, minimal realisation and power series matching methods.¹ However the general case of mixed $[n-1, n]_{2n-K}^K$ p.a.s for any K has not received much attention perhaps because its importance has not been appreciated enough and its general formula seemed to lead to entangled algorithms. The purpose of this letter is to introduce a simple formulation to complete $[n-1, n]_{2n-K}^K$ p.a.s for any n and $K = 0, 1, \dots, 2n$ and to emphasise its significant importance in model reduction for closed loop system design.

New formulation for complete p.a.s: For $G(s)$ of eqn. 3 to be an $[n-1, n]_L^K$ p.a. of $H(s)$ it is required that its first terms of expansion about $s = 0$ and $s = \infty$ are identical to the L and K first terms of eqns. 1 and 2, respectively. A significant reduction in the computational effort and a formulation that is easy to apply can be obtained if the involved time and Markov parameters are redefined in the following order:

$$F_i = M_{K-i}, \quad F_{K+j} = H_j \\ (i = 0, 1, \dots, K-1, \quad j = 0, 1, \dots, L-1) \quad (5)$$

It then can be verified that the various $[n-1, n]_L^K$ p.a.s may be obtained by the next two steps:

(i) Solution of the set of n equations for the denominator coefficients

$$\begin{bmatrix} F_{n-1} & F_{n-2} & \dots & F_0 \\ F_n & F_{n-1} & \dots & F_1 \\ \vdots & \vdots & \ddots & \vdots \\ F_{2n-2} & F_{2n-3} & \dots & F_{n-1} \end{bmatrix} \begin{bmatrix} \beta_1 \\ \beta_2 \\ \vdots \\ \beta_n \end{bmatrix} = \begin{bmatrix} -F_n \\ -F_{n+1} \\ \vdots \\ -F_{2n-1} \end{bmatrix} \quad (6a)$$

The special Toeplitz structure of this set can be used to obtain the solution iteratively (within $O(n^2)$ multiplication).²

(ii) Calculation of the numerator coefficients α_k , $k = 0, 1, \dots, n-1$

$$\alpha_k = \begin{cases} \sum_{i=0}^k H_i \beta_{k-i} & K \leq n \\ \sum_{i=k+1}^n M_{i-k} \beta_i & K \geq n \end{cases} \quad (6b)$$

Application of complete p.a.s in feedback design: A property of Padé-type reduced models that is useful in closed loop system design is discussed in References 3 to 5. It is shown there that, for a large class of constant state and dynamic output feedback laws, the closed loop transfer functions of the model and the system are related, in the Padé sense, in a similar way to that of the corresponding open loop transfer functions. Thus, taking for example output feedback, if $G(s)$ is an $[n-1, n]_L^K$ p.a. of $H(s)$ then $G_c(s) = G(s)[I + F(s)G(s)]^{-1}$ and $H_c(s) = H(s) \times$

$[I + F(s)H(s)]^{-1}$ have identical first L and K terms of expansions about $s = 0$ and $s = \infty$, respectively. It is reasonable to expect that the more parameters are shared in common by the two closed loop transfer functions the closer is the approximated design to the optimal and the better are the tracking properties between the two closed loop systems. The models obtained by the formulation of this letter have the maximum possible matched system closed loop moments for a model of a given degree. Given a high order stable system it is not certain that all the m reduced models of order n are also stable but any such obtained stable model preserves twice the number of time and Markov parameters that are preserved by a partial p.a. model of similar degree that ensure stability.³ Thus, the search for an appropriate complete p.a. reduced order model may prove to be superior for improved tracking and near optimal feedback designs that are based on reduced models. The given formulation provides a simple tool that can be applied to obtain all possible complete p.a.s of a given order.

Example: Consider second order models for the sixth order system of Reference 6 whose transfer function is

$$H(s) = \{(10^5 + 140100s + 69140s^2 + 14069s^3 + 1014s^4 + s^5)/(10^6 + 2220000s + 1454100s^2 + 248420s^3 + 14541s^4 + 222s^5 + s^6)\} \quad (7)$$

The $[1, 2]_3^2$ p.a. is unstable. Using $F_0 = M_1 = 1$, $F_1 = H_0 = 0.1$, $F_2 = H_1 = 0.0810$, $F_3 = H_2 = 0.1055$ we find the $[1, 2]_3^3$ p.a. which is stable and is given by $G^4(s)$ (upper index is used to indicate the number of matched parameters)

$$G^4(s) = \frac{0.1 + 0.0535s}{1 + 1.3541s + 0.0535s^2} \quad (8)$$

The method of Reference 6 searches for stable reduced order models by retention of some of the original system poles and completion of the models by partial p.a. It yields the following model that retains a pole at -100 (and matches H_0, H_1, H_2):

$$G^3(s) = \frac{0.1 + 0.0486s}{1 + 1.3045s + 0.0129s^2} \quad (9)$$

Applying the method of Reference 3 that assures stability preservation results in (but now only H_0, H_1 are matched)

$$G^2(s) = \frac{0.1 + 0.1310s}{1 + 2.22s + 1.3422s^2} \quad (10)$$

The closed loop transfer function for system and models $H_c(s) = H(s)[I + F(s)H(s)]^{-1}$ and

$$G_c^i(s) = G^i(s)[I + F(s)G^i(s)]^{-1}$$

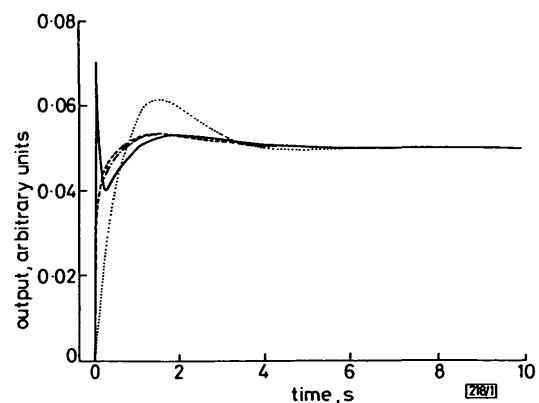


Fig. 1 Closed loops unit step responses

$$\begin{cases} \text{—} & H_c(s) \\ \text{- - -} & G_c^4(s) \\ \text{. . .} & G_c^3(s) \\ \text{- . - .} & G_c^2(s) \end{cases}$$

for $i = 2, 3, 4$ and $F(s) = (S + 10)/(s + 1)$ have been calculated and their step responses are compared in Fig. 1.

Y. BISTRITZ

27th May 1980

Tel-Aviv University
School of Engineering
Ramat Aviv, Israel

References

- 1 DECOSTER, M., and VAN CAUWENBERGHE, A. R.: 'A comparative study of different reduction methods', *J. A. (Belgium)*, 1976, 17, pp. 68-74, pp. 125-134
- 2 ZOHAR, S.: 'Toeplitz matrix inversion: the algorithm of W. F. Trench', *J. Assoc. Comput. Mach.*, 1971, 10, pp. 592-601
- 3 HUTTON, M. F.: 'Routh approximation method for high order linear systems'. Ph.D. dissertation, Polytechnic Institute of NY, 1974
- 4 HICKLIN, J., and SINHA, N. K.: 'Near optimal control using reduced order models', *Electron. Lett.*, 1976, 12, pp. 259-260
- 5 SHAMASH, Y.: 'Closed loop feedback systems using reduced order models', *ibid.*, 1976, 12, pp. 638-639
- 6 SHAMASH, Y.: 'Stable reduced order models using Padé type approximations', *IEEE Trans.*, 1974, AC-19, pp. 615-616

0013-5194/80/140563-03\$1.50/0

ELECTRICAL CONDUCTION IN METAL/IMPLANTED SiO_2/Si STRUCTURES

Indexing terms: Insulating materials, M.O.S. structures

Direct current/voltage relationships for m.o.s. capacitors are measured as function of oxide doping. Uniform P^+ doping is obtained by means of multiple ion implantation. A close relationship between oxide defects, conduction and memory switching is then emphasised.

The role of impurities in the thermally grown silicon dioxide films of metal-oxide-semiconductor (m.o.s.) structures has been a topic of continuing interest for both physicist and technologist. This letter reports how the ion implantation of an SiO_2 film can modify the electrical conductivity of the structure.

Many authors¹⁻³ have related the forming of negative resistance and memory switching in m.o.s. capacitors to the impurity content of the oxide film. However, a correlation between such forming and the conduction mechanism before it has not been emphasised because of reproducibility problems. In this work we have introduced a controlled amount of phosphorus ions P^+ into the oxide film to dope it uniformly over its entire width.

The n -type silicon wafers used here had $\langle 111 \rangle$ surfaces and resistivity of about $2 \Omega\text{cm}$. After a classical chemical cleaning, the oxide films were thermally grown at 1000°C in wet oxygen to a nominal thickness of 100 nm. The wafers were then annealed in dry nitrogen at the same temperature for 20 min. The doping of the oxide was carried out by means of multiple ion implantation at different energies and doses. The implantation parameters were calculated using the Gibbons theory⁴ so that a uniform profile could be obtained. For example, the following table gives the parameters used to get a doping of $5 \times 10^{21} \text{ P}^+/\text{cm}^3$ (wafer 2):

Energy (keV)	80	42	23	12
Dose $\times 10^{-16}$ (cm^{-2})	3.6	1.4	0.7	0.45
R_p (nm)	86	50	26	14
S (nm)	21.5	13.2	8.4	5.1

where R_p and S are the projected range and the standard deviation of the Gaussian profile corresponding to a given energy and dose. Two other wafers were doped using the same ener-

gies but with doses such that concentrations of 10^{21} cm^{-2} (wafer 1) and 10^{22} cm^{-2} (wafer 3) were obtained. Before the metallic electrode evaporation, about 5 nm of the oxide surface was stripped off since this layer is generally of very defective nature. Molybdenum was electron-beam-evaporated over the oxide to a thickness of about 100 nm. Such an inert electrode was used to avoid any uncontrolled metallic impurities being diffused or injected into the oxide from the electrode.⁵

1 μm of aluminium was then evaporated on to protect the underlying molybdenum against oxidation. Square capacitors of three different areas were patterned by photolithography (smallest area was $100 \times 100 \mu\text{m}^2$ and the others were 4 times and 16 times this area). The terminated structures were not annealed after metallisation.

The electrical conduction through the oxide layer was measured with the sample in a shielded box containing dry air to minimise surface leakage currents between adjacent capacitors. The back of the wafer was painted with silver to improve the contact with the support. Contact to the metallic electrode was made by means of a spring-loaded tungsten probe. The support temperature can be varied between -40°C and 80°C using a thermoelectric module (Peltier effect) and the temperature was measured by a thermocouple. Currents as small as 10^{-15} A were measured by means of a Keithley electrometer.

The measurements of the direct current/voltage I/V curves were carried out with the metal contact biased positively, and typical room temperature characteristics are shown in Fig. 1 for the three wafers used. As can be seen, the I/V relationship depends on the doping level of the oxide film.

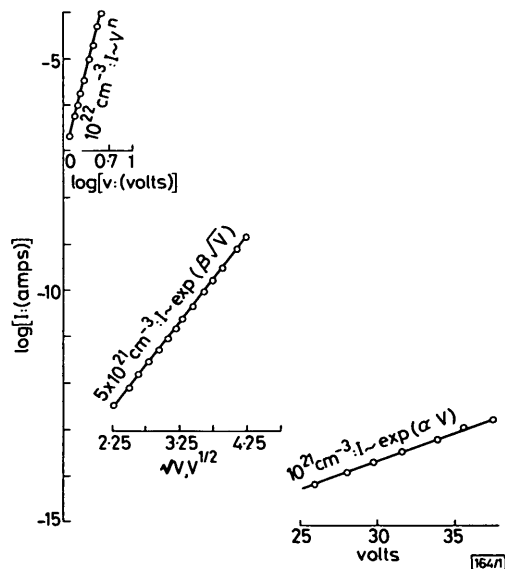


Fig. 1 Virgin state conduction with implanted P^+ doping as parameter

Wafer 1 (low doping) shows an exponential dependence of current on voltage at high fields, as is often observed in pure SiO_2 films³ at fields lower than the onset of Fowler-Nordheim injection. Such an exponential relationship might be explained by a space charge limited current with charge trapping within the oxide film. These 'low doped' samples do not show any switching phenomenon other than permanent breakdown.

Wafer 2 (medium doping) shows an exponential dependence of current on the square root of the voltage up to some critical field at which the capacitor switches to a high conducting state (electrical forming). This high conducting state is ohmic in nature and is not a permanent state. It can be removed by forcing a high density of a current pulse in the switched 'on' capacitor. The unformed conduction mechanism corresponds to either Schottky or Poole-Frenkel emission.⁶ Only the temperature dependence of the conduction characteristics can allow us to decide whether the conduction is limited by the first or by the second mechanism. We have used the method given by Hill⁷ in which the curves of $IT^{-4} \exp(E/kT)$ against $V^{1/2}T^{-1}$ for different temperatures T (K) coincide, resulting in a single normalised curve only if the conduction is limited by a Poole-Frenkel emission. Here I is the current (in amps), V is the applied potential in volts and k is the Boltzmann constant.